Patient-derived precision cut tissue slices from primary liver cancer as a potential platform for preclinical drug testing

Ravi Jagatia,[a,b,h] Ewald J. Doornebal,[a,b,h] Una Rastovic,[a,b] Nicola Harris,[a,b] Moyosoreoluwa Feyide,[a,b] Anabel Martinez Lyons,[c] Rosa Miquel,[d] Yoh Zen,[d] Ane Zamalloa,[e] Farooq Malik,[e] Andreas Prachalias,[e] Krishna Menon,[e] Luke Boulter,[c,f] Simon Eaton,[g] Nigel Heaton,[e] Sandra Phillips,[a,b] Shilpa Chokshi,[a,b,i] and Elena Palma[a,b,*,i]

[a]The Roger Williams Institute of Hepatology, Foundation for Liver Research, 111, Coldharbour Lane, London SE5 9NT, United Kingdom
[b]Faculty of Life Sciences and Medicine, King's College London, London WC2R 2LS, United Kingdom
[c]MRC Human Genetics Unit, Institute of Genetics and Cancer, Western General Hospital, University of Edinburgh, Crewe Road, Edinburgh EH4 2XU, United Kingdom
[d]Liver Histopathology Laboratory, Institute of Liver Studies, King's College Hospital, Denmark Hill, London SE5 9RS, United Kingdom
[e]Institute of Liver Studies, King's College Hospital and King's College London, Denmark Hill, London SE5 9RS, United Kingdom
[f]Cancer Research UK Scottish Centre, Institute of Genetics and Cancer, Western General Hospital, Crewe Road, Edinburgh EH4 2XU, United Kingdom
[g]Great Ormond Street Institute of Child Health, University College London, 30 Guilford Street, London WC1N 1EH, United Kingdom

Summary

Background The exploitation of anti-tumour immunity, harnessed through immunomodulatory therapies, has fundamentally changed the treatment of primary liver cancer (PLC). However, this has posed significant challenges in preclinical research. Novel immunologically relevant models for PLC are urgently required to improve the translation from bench to bedside and back, explore and predict effective combinatorial therapies, aid novel drug discovery and develop personalised treatment modalities.

Methods We used human precision-cut tissue slices (PCTS) derived from resected tumours to create a patient-specific immunocompetent disease model that captures the multifaceted and intricate heterogeneity of the tumour and the tumour microenvironment. Tissue architecture, tumour viability and treatment response to single agent and combination therapies were assessed longitudinally over 8 days of *ex vivo* culture by histological analysis, detection of proliferation/cell death markers, ATP content via HPLC. Immune cell infiltrate was assessed using PCR and immunofluorescence. Checkpoint receptor expression was quantified via Quantigene RNA assay.

Findings After optimising the culture conditions, PCTS maintained the original tissue architecture, including tumour morphology, stroma and tumour-infiltrated leukocytes. Moreover, PCTS retained the tumour-specific immunophenotype over time, suggesting the utility of PCTS to investigate immunotherapeutic drug efficacy and identify non-responsiveness.

Interpretation Here we have characterised the PCTS model and demonstrated its effectiveness as a robust preclinical tool that will significantly support the development of successful (immuno)therapeutic strategies for PLC.

Funding Foundation for Liver Research, London.

Keywords: Hepatocellular carcinoma; Intrahepatic cholangiocarcinoma; Immune checkpoint; Tumour culture; Immunotherapy

Introduction

Primary liver cancers are currently in the top two causes of cancer-related deaths worldwide, with incidence continuing to increase year on year.[1] The main subtypes of primary liver cancer include hepatocellular carcinoma (HCC, 80–85%), cholangiocarcinoma (CCA, 10–15%)

---

*Corresponding author. The Roger Williams Institute of Hepatology, Foundation for Liver Research, 111, Coldharbour Lane, London SE5 9NT, United Kingdom.
E-mail address: e.palma@researchinliver.org.uk (E. Palma).
[h]Equal contribution.
[i]Joint senior authors.

Research in context

Evidence before this study
Primary liver cancer is characterised by multifactorial processes and presents diverse and type-specific features. The heterogeneity among patients and tumours makes liver cancer complex to study and recapitulate at a preclinical stage. In addition, the undeniable flaws in current experimental models have dramatically hindered the understanding of the pathobiology of these cancers and led to multiple failed clinical trials.

Added value of this study
Here we describe an organotypic and immunocompetent model based on the *ex vivo* culture of patient-derived cancer explants (Precision Cut Tissue Slices) originated from

hepatocellular carcinoma, intrahepatic cholangiocarcinoma and mixed phenotype. The novelty is on the optimisation and standardisation of culture conditions and in the longitudinal assessment for an extended time of the immune component, tumour-specific histologicaland molecular features that are critical for reliable drug development.

Implications of all the available evidence
The PCTS model will benefit preclinical and clinical research for primary liver cancer: it will allow reliable testing of novel therapeutic approaches, the identification of non-response and the potential development of personalised medicine approaches to improve the clinical management of liver cancer patients.

and mixed phenotype (HCC-CCA, 0.4–14.2%),[2] which present diverse and type-specific characteristics. HCC is a prototypical inflammation-related cancer mostly associated with chronic liver injury, inflammation and cirrhosis. Immunologically, HCC can be stratified based on lymphocyte infiltration (i.e., hot/cold), expression of inhibitory immune checkpoint receptors/ligands [(i.e., Programmed cell death protein 1/Ligand 1 (PD-1/PD-L1), Cytotoxic T-lymphocyte-associated protein 4 (CTLA-4)], and other immunosuppressive factors.[3–8] Whilst intrahepatic CCA (iCCA) is a distinct biliary cancer, inflammation and checkpoint receptors (CRs) also seem to play key roles.[9,10] Multifactorial processes underlying tumourigenesis and their heterogeneity, make liver cancers complex to study and to recapitulate at a pre-clinical stage.

As with other cancers, immunotherapy has revolutionised the treatment landscape for liver cancers. Since the 2010s, clinical studies have been testing the safety and efficacy of immune-checkpoint inhibitors (CPIs) in advance stage HCC.[11–13] Even though single-agent regimens (i.e., PD-1 inhibitors) have failed to significantly improve survival compared to Sorafenib,[11,13] encouraging results have been obtained with CPIs in combination with anti-angiogenic therapies.[14] These have led to the selection of atezolizumab (anti PD-L1) and bevacizumab (anti-VEGF-A) as the standard of care for advanced disease. In the context of CCA, treatment options are scarce; however, combination therapies with CPIs have recently shown promising results but need further study.[10] Notably, detailed investigations of the additive or synergistic effects of treatments in the clinical pipeline are lacking. Certainly, drug development for HCC has been hindered by the challenge of translating experimental studies from bench to bedside, leading to multiple failed clinical trials.[15] Whereas for CCA, a lack of understanding regarding the (immuno) biology of this cancer has impeded therapeutic advancement.

In addition, there is an urgent need for accurate, immunocompetent liver cancer models that capture the human disease to identify efficacious regimens, particularly given the high rates of non-response to CPIs (<30%)[10,16] to foster reliable drug development. These models also need to be rapidly available to keep pace with a highly evolving therapeutic landscape. To date, research and drug discovery for liver cancer has relied heavily on 2-dimensional culture systems and animal models, including patient-derived xenograft or genetically engineered mice.[17–19] Unfortunately, while these are established, they present major flaws. They fail to recapitulate the patient-specific tumour microenvironment (TME) and the relevant background liver disease, that drives inflammation and immune exhaustion, or lack essential features of the human immune system relevant for investigating immunotherapies. These limitations contribute to the observed difference between the preclinical and clinical successes of emerging (immuno)therapeutics.[20,21] More advanced approaches using organoids have recently been reported for HCC, CCA and HCC-CCA.[22,23] However, like all cell-based models, organoids are inherently susceptible to clonal selection after isolation of the tumour cells[24] and lack the underlying TME and native immune system. A relevant addition to 3D models is represented by the culture of precision-cut tissue slices (PCTS), which preserve the structure and cellular heterogeneity of the tissue of origin and have successfully been used to recapitulate the cellular and histological characteristics of the liver.[25–28] Recently we have demonstrated that tumour slices derived from neuroendocrine liver metastasis are immunocompetent and can be cultured for up to 14 days without losing viability.[29]

Here, we describe the development and characterisation of a PCTS disease model for primary liver cancer that captures the patient-specific heterogeneity. Firstly, we focused on the optimisation of the slice culture conditions (i.e., oxygen levels) required to preserve

viability and tumour proliferative characteristics and showed that tumour slices derived from HCC and iCCA (n = 16) were viable for at least 8 days. Further, we investigated critical immunological features of the PCTS in culture and showed that they retain the unique patient-specific immune component, including the resident populations, characterised by an infiltrated but suppressed immunity. Finally, we demonstrated the utility of PCTS as a model for personalised drug screening of immunotherapeutic strategies.

Methods

Patient recruitment and ethics statement

Patients undergoing partial hepatectomy, as treatment for primary liver cancer, were enrolled and written informed consent was obtained for all the subjects involved in this study (Table 1 for clinical characteristics). This study was conducted according to the Declaration of Helsinki principles and approved by the local Research Ethics Committee established by the Health Research Authority (REC reference 17/NE/0340; IRAS project ID 222302). Samples were collected from October 2018 to April 2023. Patient recruitment included both males and females in an unbiased manner.

Generation of precision cut liver tumour slices

PCTS were obtained and cultured as previously described and illustrated in Fig. 1.[29–31] The tissue specimens were flushed immediately after resection with sterile ice-cold organ preservative University of Wisconsin solution (Bridge of Life, UW). Tissue cores were cut from the tumour and surrounding tissue using a 5 mm cylindrical hollow drill bit and tissue coring press

(Alabama R&D, MD5000), and 250 μm thick tissue slices were cut using a tissue slicer (Alabama R&D, MD6000). Krebs–Henseleit solution (2.5 mM $CaCl_2$, 118 mM NaCl, 5 mM KCl, 1.1 mM $MgSO_4$, 1.2 mM KH_2PO_4, 25 mM $NaHCO_3$ from Merck, 25 mM D-Glucose, 9 mM HEPES from Fisher Scientific) pH 7.42 saturated with carbogen (95% O_2/5% CO_2) was used as slicing buffer. All tissue slices were incubated in 12 well plates (Nunc) under 70 rpm orbital shaking in a humidified incubator, 95% O_2/5% CO_2, 37 °C, for 2 h (recovery step) in 1.5 mL supplemented William's Medium E (WME) [William's E Medium (Life Technologies, 32551-020), penicillin/streptomycin (Life Technologies, 15140-122), 2 mM glutamine (Life Technologies, 25030-024), ITS (10 mg/L Insulin +5.5 mg/L Transferrin +6.7 μg/L Sodium selenite) (Life Technologies, 41400-045), 1 nM epidermal growth factor (Life Technologies, PHG0311), 5% Human AB serum (Cambridge Bioscience, 515-HI-GI-AB-100), 100 nM glucagon (Merck, G2044-1MG) and 1 μM corticosterone (Merck, 27840-100MG)]. The slice culture medium was replaced after the recovery step and subsequently every day until the end of the culture. After recovery, slices were kept at 37 °C with 95% O_2/5% CO_2 (carbogen) or moved into 5% CO_2 (atmospheric) incubation in accordance to the experimental plan.

Lactate dehydrogenase (LDH)

Supernatants were collected in triplicate for each time-point and frozen at –80 °C for batch analysis. LDH activity was measured in the slice culture supernatants using the CytoTox 96 Cytoxicity Assay colorimetric assay (Promega, G1780) according to the manufacturer's instructions. Tissue slices, collected at the start of the

Patient (PCLS-XXX)	Sex	Age	Ethnicity	Primary	Underlying aetiology	Previous treatment	Grade	Fibrosis
024	**F**	**73**	**Caucasian**	**CCA**	**N/A**	**N/A**	**G3**	**F1–F2**
039	M	70	Caucasian	HCC	N/A	N/A	G2	F4
056	**M**	**58**	**Caucasian**	**HCC**	**N/A**	**TACE; SIRT; PvE; ablation**	**G3**	**Cirrhosis**
098	M	83	Caucasian	HCC & CCA	N/A	Left hemicolectomy; adjuvant chemo	G3	F0
099	F	61	Caucasian	HCC	CLD	N/A	G2	F3
100	F	63	Caucasian	CCA	Past HCV	N/A	G3	F1–F2
107	F	66	Caucasian	HCC	N/A	N/A	G3	F1–F2
110	F	52	Caucasian	HCC	N/A	N/A	G1	F1
141	M	82	Caucasian	HCC	N/A	N/A	G2	F1
166	M	75	Caucasian	CCA	NASH CLD	MVA	G2	F3
168	M	70	Caucasian	HCC	NAFLD	N/A	G3	F0–F1
202	M	77	Black, African	HCC & CCA	N/A	Left lateral hepatectomy	G1	F0
212	M	71	Caucasian	HCC	N/A	N/A	G2	F3–F4
213	F	74	Asian	HCC	N/A	Right hemihepatectomy	G2	F1
222	F	80	Caucasian	CCA	N/A	Left hemihepatectomy; caudate lobe resection	G3	N/A
255	M	80	South Asian	HCC	N/A	N/A	G2	F0

Clinical characteristics of the donors of the tissue specimens utilized to produce precision cut liver tumor slices (PCTS). Stromal tumors with no viable tumor epithelium are indicated in bold. Indicated previous treatments are in relation to liver cancer. HIV or Hepatitis C/B positive patients were excluded from the study.

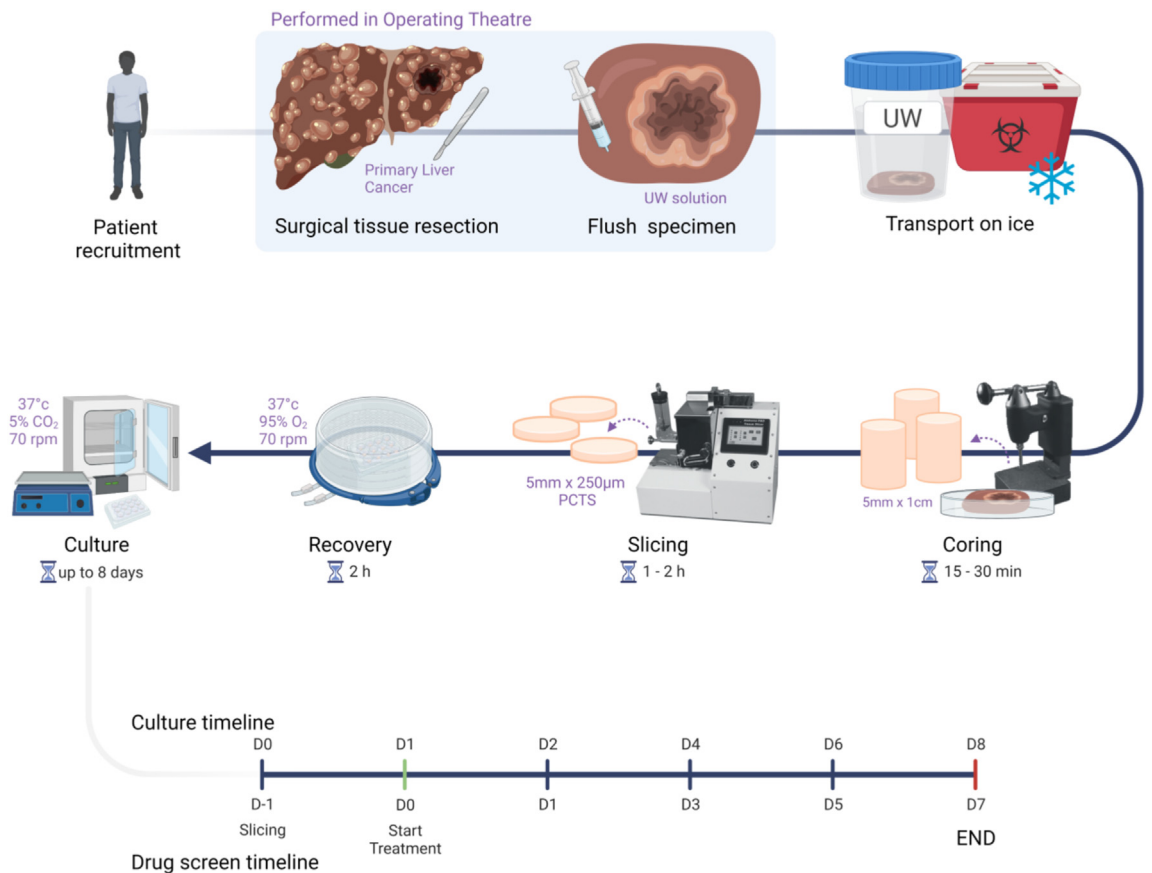*Table 1*: Patient clinical information.

Fig. 1: Schematic diagram highlighting the key steps of PCTS production from human tumour explants. The timeline illustrated in the final row shows: the overall culture timeline (8 days) (top) with the corresponding drug screening experiment timeline (bottom), the collection timepoints indicate the duration of drug exposure. In drug screening experiments, slice treatment starts after 1 day in culture (indicated in green). All subsequent graphs representing longitudinal data are labelled "Time in culture" or "Time post treatment" in concordance with this schematic.

culture and homogenised, were used as positive controls to determine the total LDH content per mg tissue present. Homogenisation was performed using a Precellys homogeniser (Bertin instruments); program: 2 cycles × 25 s, 5500 rpm, 30 s pause.

Adenosine nucleotides/energy charge
Intracellular adenosine and adenosine mono-/di-/triphosphate (AMP, ADP and ATP, respectively) were quantified in liver slice homogenates by High Performance Liquid Chromatography (HPLC) to assess intracellular ATP content (viability) and adenylate energy charge (metabolic capacity/state) as previously described.[29]

Histology/embedding
Tissue slices were fixed in 10% neutral buffered formalin (Fisher Scientific, 13191184) v/v overnight at 4 °C. Fixed tissue slices were either cryo-protected by placing the slices in 30% w/v sucrose (Merck, S0389-500G) at 4 °C and embedded in 7.5% porcine gelatin (Merck) w/v +15%

sucrose w/v in PBS at 37 °C. With blocks being frozen in dry-ice cooled isopentane (Fisher Scientific, 10468030) and stored at −80 °C until cryosectioning at 7 or 10 μm as described in[29] or pre-processed for paraffin embedding: dehydrated with ethanol (VWR, 20821.365), cleared with xylene (Fisher Scientific, 10385910) and embedded in paraffin (VWR, 361427G). Paraffin blocks were cut using a microtome at a thickness of 4 μm. Where indicated, adjacent sections were stained for different histological or fluorescent markers to allow for comparison between panels.

H&E staining was performed using Harris haematoxylin (Fisher Scientific, 12647926). After dedifferentiation, sections were stained with eosin (Merck, HT110116), dehydrated and mounted with DPX mounting medium (Merck, 1005790500). Images were taken at 20× magnification. For immunofluorescence, sections were permeabilised and blocked with 0.1% v/v Triton X-100 (Merck, T8787) and 1% BSA (Merck, A9418) v/v in PBS for 45 min at room temperature.
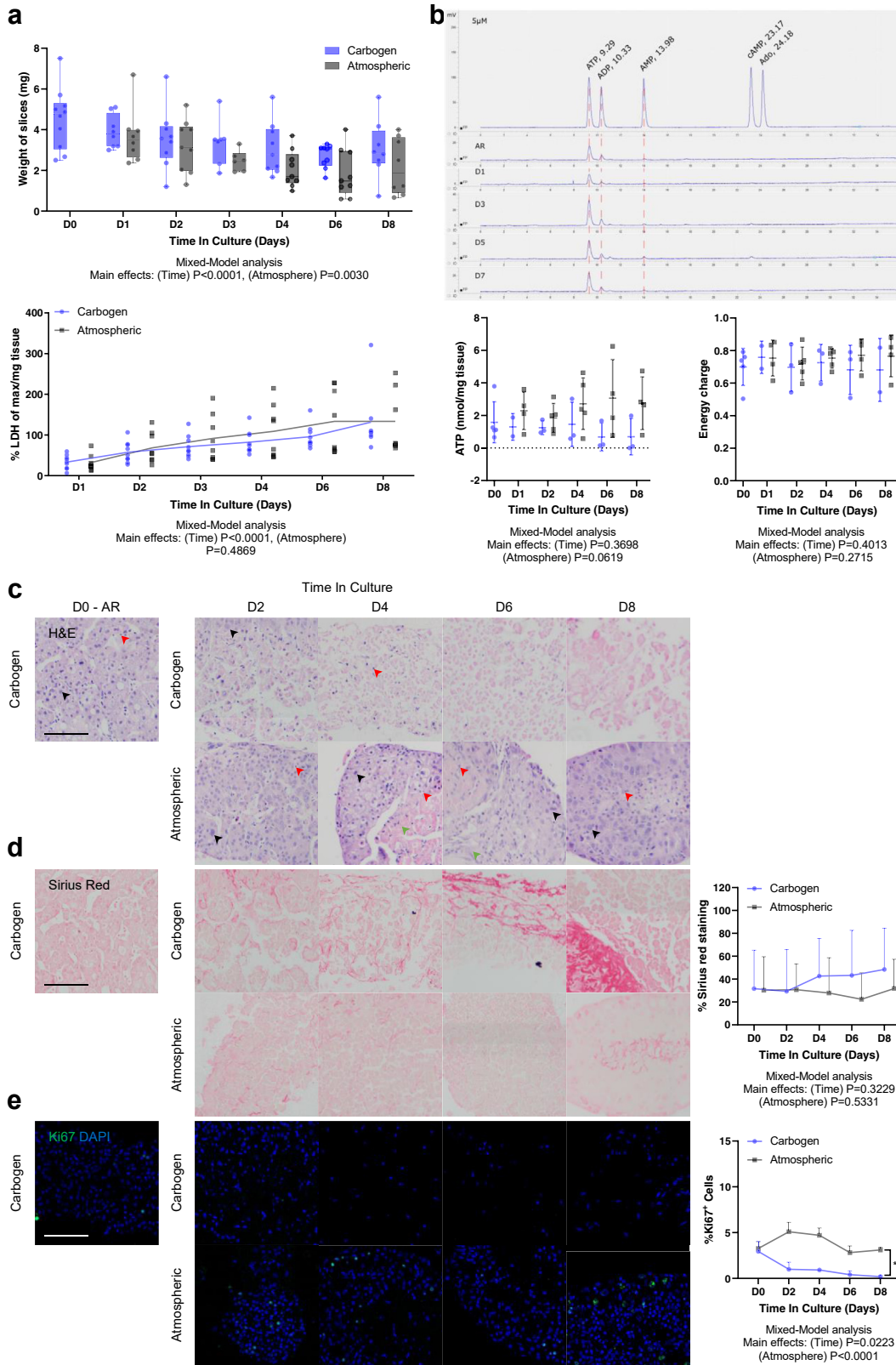
Primary antibodies were diluted in blocking buffer (anti-Ki67, 1:500; anti-CD3, 1:500; anti-CD45 1 µg/mL) and incubated overnight at 4 °C. Secondary antibodies were applied the next day for 45 min at room temperature (full list with antibody details in Supplementary Table S1). Phalloidin toxin 1:1000 (Abcam, ab176757) staining for actin was performed together with the secondary antibody staining step. For the evaluation of apoptosis, tissue sections were stained using Dead-end Fluorometric TUNEL Kit (Promega, G3250). All samples were mounted with Fluoroshield mounting medium with DAPI (Abcam, ab104135). Images were collected using a Cytation 5 imaging system (BioTek) at 10× magnification or Olympus Fluorescence Microscope BX431 using UPlan FL N 20× and 40× objectives. Post-imaging analysis and quantification was performed in ImageJ using automated scripts. Any background reduction, brightness or contrast modifications were applied across a complete image dataset.

Gene expression analysis of CRs in PCTS
The gene expression of a panel containing *BTLA, CD27, CD274* (PD-L1), *CD28, CD80, CTLA-4, HAVCR2* (Tim-3), *IDO1, LAG3, PDCD1* (PD-1), *PDCD1LG2* (PD-L2), *TNFRSF14* (HVEM), *TNFRSF18* (GITR), *TNFRSF9* (CD137) and housekeeping genes *PPIB, RPLP0, RPS29, HPRT1* was quantified using the QuantiGene® Plex 2.0 platform (ThermoFisher Scientific). Tissue slices for QuantiGene analysis were placed in 50 µl of Allprotect Tissue Reagent (Qiagen, 76405) according to the manufacturer's instructions and stored at –80 °C. All samples for the QuantiGene assay were <5 mg and processed simultaneously using the QuantiGene Sample Processing Kit (ThermoFisher Scientific, QS0104). In short, tissue slices were thawed on ice and placed in RNAse/DNAse tubes with 1.4 mm ceramic beads (Bertin Instruments, P000933-LYSK0-A), 600 µl homogenisation solution (provided with the kit) and 6 µl proteinase K (ThermoFisher, QS0511). Homogenization was performed at 4 °C using a Precellys homogeniser (Bertin Instruments, P000062-PEVO0-A); program 2 cycles × 15 s, 5000 rpm, 1-min pause on ice. Tissue homogenates were further processed according to the manual and used undiluted for the QuantiGene assay. All samples were detected at the same time on a Luminex MAGPIX instrument (Invitrogen, APX1042). The assay was performed according to the QuantiGene plex gene expression assay user guide provided with the custom QuantiGene panel (Invitrogen, QP1013). Data were analysed in the QuantiGene Plex Data Analysis cloud APP (Thermo). Normalised expression was calculated by normalising the MFI of the gene of interest with the geometric mean of the housekeeping genes. For each sample, fold change in gene expression was calculated against patient matched surrounding tumour-free liver tissue which was collected at the time of slicing and stored in Allprotect tissue reagent until processing.

Innate and Adaptive Immune Responses PCR array
Tissue slices were preserved in Allprotect Tissue Reagent (Qiagen, 76405) and stored at –80 °C until processing. RNA, DNA and protein content were isolated with AllPrep DNA/RNA/Protein Mini Kit (Qiagen) according to manufacturer's instructions. cDNA was synthesised with RT2 First Strand Kit (Qiagen) and analysed with Innate and Adaptive Immune Responses RT2 Profiler PCR Array (Qiagen) with RT2 SYBR® Green qPCR Mastermix. qPCR microarray for Human Innate & Adaptive Immune Responses (Qiagen, 330231 PAHS-052ZA) was run on ABI 7500 Real-Time PCR System with an initial denaturation step at 95 °C for 10 min followed by 40 cycles of denaturation at 95 °C for 15 s and annealing/extension at 60 °C for 60 s. Gene expression fold change was calculated by determining the ratio of mRNA levels to control values using the ΔCt method ($2^{-\Delta\Delta Ct}$). Data analysis and clustering were performed using Qiagen's online web analysis tool and guidelines by the manufacturer.

Drug treatments
PCTS were exposed to the following drugs and analysis was performed at the timepoints indicated in Fig. 1: doxorubicin (Doxo, Selleck chem, S1208), 2 µM[32,33]; regorafenib (Selleck chem, S5077), 5 µM[34,35]; nivolumab (Selleck chem, A2002), 2.6 nM[36]; anti-PD-1 blocking IgG (R&D, MAB10864), 0.46 µg/mL; ipilimumab (Selleck chem, A2001), 0.5 nM[37]; bevacizumab (Selleck chem, A2006), 0.5 nM[38]; atezolizumab (Selleck chem, A2004),

Fig. 2: Effect of culture time and oxygen levels on PCTS: tumour slices from primary liver cancer better maintain the original tumour characteristics when cultured in atmospheric conditions. a | Slice weight (top) and LDH release (bottom) were longitudinally evaluated in PCTS cultured for 8 days in atmospheric (black) vs carbogen (blue) conditions; mean ± SD, n_{pt} = 9, each dot corresponds to n_{PCTS} = 3. b | Weight-adjusted ATP and energy charge were longitudinally quantified in tumour slices cultured in atmospheric (black) vs carbogen (blue) conditions; mean ± SD, n_{pt} = 4, each dot corresponds to n_{PCTS} = 3. The upper panel shows a representative HPLC chromatogram with peaks at retention times corresponding to the different adenosine nucleotides. c | Representative images from pt 255 of H&E staining of tumour slices cultured in carbogen and atmospheric conditions [arrows indicate epithelial cells (black), the stromal compartment (green) and non-parenchymal tumour cells (red)]. d | Representative images from pt 255 of Sirius red collagen staining in PCTS cultured in carbogen vs atmospheric conditions and corresponding quantification of collagen fraction; mean ± SD, n_{pt} = 4, each dot corresponds to n_{PCTS} = 3. e | Representative images from pt 255 of Ki67/DAPI staining in PCTS (Ki67+ nuclei in green) and corresponding quantification of proliferating cells; mean ± SD, n_{pt} = 4, each dot corresponds to n_{PCTS} = 3. All scale bars: 100 µm. AR: after recovery.
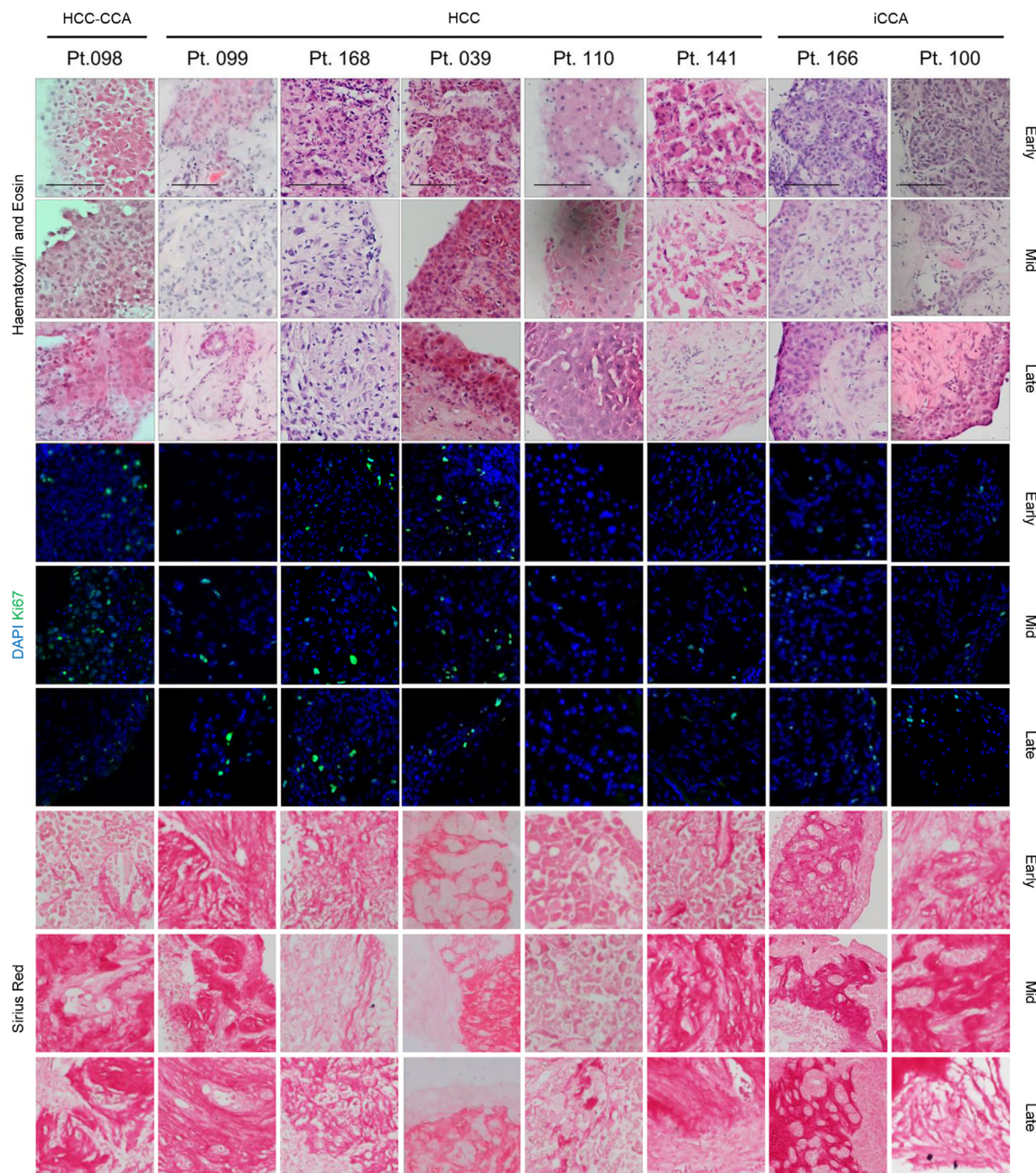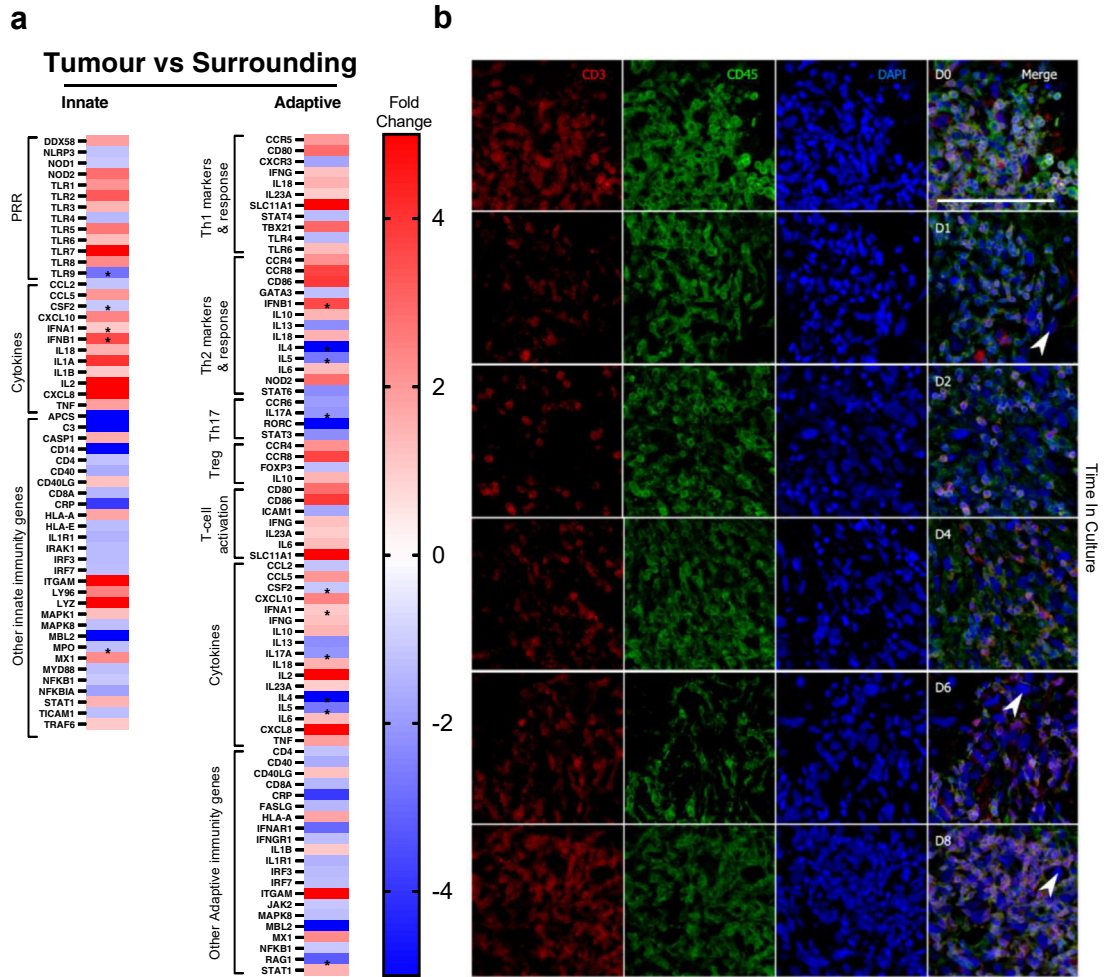
Fig. 3: Effect of PCTS culture on the original tumour characteristics: tissue slices from HCC/iCCA maintain histological features, proliferative capacity and extracellular matrix organisation. Top 3 rows: histological evaluation using H&E staining; middle 3 rows: evaluation of tumour cell proliferative capacity using Ki67 staining; bottom 3 rows: evaluation of extracellular matrix using Sirius red staining, Scale bars: 100 μm. Labels early, mid and late refer to days 0–1, 3–4 and 6–8 of culture, respectively.

0.5 nM.[39] Drugs were dissolved in PBS or DMSO as instructed by the manufacturer.

Statistical analysis
Multiple replicate slices or supernatants from each patient-derived culture were utilised and compared across conditions and timepoints. If necessary, log-transformed raw data were utilised for the statistical analysis. Day 0 was plotted but excluded from statistical analyses. For continuous variables, Repeated-Measures Two-way ANOVA with Holm-Sidak's post-hoc correction for paired samples, Two-way ANOVA model

a

Tumour vs Surrounding

b

c

Quantigene plex gene expression analysis comparing expression in tumour slices vs matched tumour-free background

adjusted for patient variability or Mixed-effects Model analysis patient matched (where applicable) with Tukey or Sidak correction for group/time-dependent cultures were used. Basic statistics were calculated with Graph-Pad Prism 9 (San Diego, CA, US), IBM SPSS Statistics 28 (Armonk, NY, US) and Microsoft Excel 2016 (Redmond, WA, US). Statistical significance was set at two-tailed $p \leq 0.05$. In all figures the meaning of the symbols are: *$p \leq 0.05$; **$p \leq 0.01$; ***$p \leq 0.001$; ****$p \leq 0.0001$.

Role of funders

The funding source did not have any involvement in study design, data collection, data analyses, interpretation, writing of report, or decision to submit it for publication.

Results

Atmospheric oxygen is required for the preservation of primary liver cancer PCTS in culture

Approximately 60–100 PCTS were derived from each tissue sample (n = 9: M_n = 6, F_n = 3) and cultured for up to 8 days (Fig. 1) in atmospheric oxygen or carbogen conditions (gold standard for liver slices) to identify the appropriate oxygenation levels required for better preservation. Parameters indicative of viability, including weight and ATP content, and cell death markers were longitudinally assessed on day 0 (after recovery step), 1, 2, 3, 4, 6 and 8 of culture. As shown in Fig. 2a, the weight of the slices was significantly affected by the duration of the culture period and the oxygen level, suggesting a difference between the two conditions requiring further investigations. The release of LDH, a marker of cell death, in slice supernatant was consistent throughout the culture. LDH release was significantly affected by the time in culture but not by the difference in oxygen concentration between atmospheric and carbogen (Fig. 2a). However, the quantification of intracellular ATP content via HPLC suggested that tissue slices were better preserved in atmospheric oxygen compared to carbogen, especially at later timepoints. Although the overall atmosphere effect did not reach significance, there was a trend indicating higher intracellular ATP concentration, normalised for the slice weight, in the tissue slices cultured in atmospheric oxygen compared to the slices cultured in carbogen (Fig. 2b). Additionally, the adenylate energy charge (AEC), used as a measurement of metabolic activity,

showed a stable trend throughout the entire culture in both oxygen environments and was not significantly affected by time in culture or oxygen concentration (Fig. 2b).

Finally, the impact of oxygen levels on PCTS was assessed by longitudinal histological analysis. The H&E staining showed that a consistent number of tumour epithelial cells (Fig. 2c) were present at all timepoints in the slices cultured in atmospheric conditions and had classical hallmarks of cancer, such as markedly enlarged nuclei. Additionally, the stromal compartment and non-parenchymal tumour cells visible at day 0, were maintained throughout the culture period. At the later timepoints, the tumour epithelium was found on the external layers, effectively surrounding the stromal compartment. This observation was consistent between all patients and different tumour types. In contrast, in slices cultured with carbogen there was a reduction of tumour epithelium after 3 days. At day 4, 6 and 8, PCTS contained no epithelial cells and only tumour stroma and non-parenchymal tumour cells persisted. Moreover, levels of fibrosis were evaluated in the tissue slices by Sirius red staining. The bright red collagen staining aligned with the stromal compartment from the H&E staining and the quantification, as % Sirius red staining, remained stable throughout the culture in the atmospheric condition. The tumour epithelial area was consistently preserved over time. Contrarily, slices cultured in carbogen had dense/darker red collagen staining at days 4, 6 and 8; however, this did not reach statistical significance (Fig. 2d).

Additionally, PCTS cultured in atmospheric oxygen maintained a consistent level of Ki67 positive cells over time, indicating maintenance of proliferative capacity. On days 4, 6 and 8, Ki67 staining was mainly present on the external layers and co-localised with the tumour epithelium as determined by nuclear morphology and the adjacently cut sections stained for H&E and Sirius red. PCTS cultured in carbogen showed a significant reduction in Ki67 staining over the duration of the culture period and little to no Ki67+ cells were observed at day 8 (Fig. 2e).

In a pilot experiment, the impact of hypoxic conditions on HCC-PCTS was evaluated (Supplementary Figure S1), but this culture did not show any advantage compared to atmospheric and therefore it was not explored further. Interestingly, when assessing only

---

Fig. 4: Effect of PCTS culture on the tumour immune component: tissue slices are immunocompetent and capture patient-specific checkpoint receptor expression. a | Heat map showing the differential gene expression of innate and adaptive markers for immunity in tissue slices from a patient with HCC comparing tumour vs matched surrounding quantified by qPCR microarray. PRR: pathogen recognition receptors. b | Representative images of immunofluorescent staining for CD3 and CD45 (T-cells) in tumour slices at day 0–8 (arrows indicate epithelial cells); n_{pt} = 3. Scale bar: 100 μm. c | Heat map showing differential gene expression of 14 checkpoint receptors comparing tumour slices cultured for the indicated time and matched tumour-free tissue slices at baseline (day 0) from patients with HCC or iCCA using a custom multiplex QuantiGene panel.
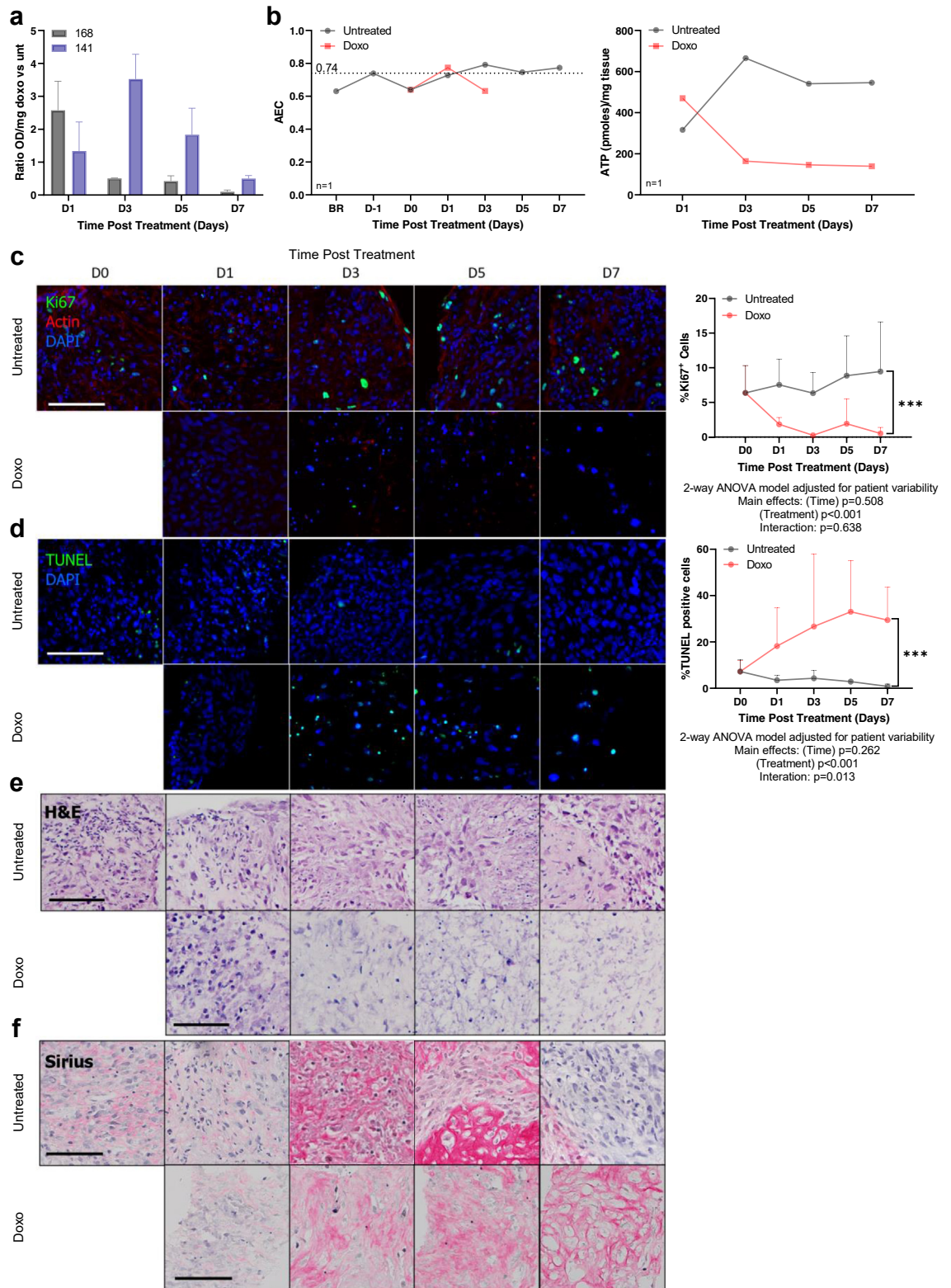
Fig. 5: **Effect of chemotherapy on PCTS: changes in tumour cell viability and proliferation are detected in tumour slices in response to doxorubicin treatment.** Untreated tumour slices (black) and PCTS exposed to 2 μM doxorubicin (red, Doxo) were collected at the indicated

atmospheric and carbogen conditions and excluding hypoxia from the statistical analysis, the % of cells with nuclear localisation of hypoxia-inducible factor 1-alpha, was significantly increased in PCTS cultured in atmospheric compared to those in carbogen (p = 0.0203, Mixed-Model analysis; Supplementary Figure S1a).

Taken together, these results suggested a superiority of the atmospheric oxygen compared to carbogen in retaining original tumour histological features and tumour proliferative capacity in slices cultured for 8 days and were in accordance with the ATP results. For this reason, further experiments were performed in the selected condition and slice cultured in atmospheric oxygen only.

Primary liver cancer PCTS maintain patient specific histology, background liver disease and molecular markers

After selecting the atmospheric condition as the most appropriate for liver cancer, a broader study was performed including additional 7 patients with HCC, iCCA or mixed phenotype. Tumour slices were cultured for up to 8 days and histological examination showed that patient-specific characteristics were maintained over time, as confirmed by the clinical histopathologist. For each patient, PCTS retained tumour epithelium, stroma, non-parenchymal tumour cells, tissue structure and proliferation rates over the duration of the culture (Fig. 3). Interpatient variability in the Ki67 levels was mirrored in the slices. PCTS with distinctive nests of tumour cells (pt 099, 039, 166 and 100) had consistent growth of tumour epithelium on the external layers (Fig. 3a). Furthermore, the patient-specific extracellular matrix organisation and the background fibrosis, as shown by Sirius red staining, was preserved throughout the culture (Fig. 3a).

PCTS retain tumour-specific immunity markers, CR expression and T-cell infiltration

After the histological evaluation of the slices in culture, we analysed the immune compartment in the tumour slices and its preservation in culture. Firstly, we quantified innate and adaptive immune markers by qPCR array analysis in PCTS from HCC tumour and matched surrounding tumour-free liver tissue (Fig. 4a). A general increase in the expression of genes associated with T-cell infiltration was detected in the PCTS (tumour vs surrounding) from the patient studied, suggesting the original tumour-specific characteristics (infiltrated but

suppressed immunophenotype)[8] were maintained in the PCTS.

The consistent presence of T-cells in tissue slices was further confirmed by detecting CD3^{+} and CD45^{+} cells by immunofluorescence (IF) longitudinally (Fig. 4b). The number of immune cells in the tumours, and consequently in the slices, including infiltrated and tissue-resident cells, is highly variable and depends on the patient and the tumour immunophenotype (Supplementary Table S3).

Finally, the gene expression of inhibitory and stimulatory CRs was longitudinally assessed in tissue slices (Fig. 4c). The CR differential expression between tumour slices at each timepoint (day 0, 2, 4, 6, 8) compared to the corresponding patient-matched surrounding background liver tissue (tumour-free) was analysed throughout the culture. The expected differences in CR expression due to patient variability (HCC 141 vs 168) and tumour type (HCC vs iCCA) were reflected in the slice model (Fig. 4c). Notably, the specific CR signatures were stably retained over the culture both in HCC and iCCA with no significant changes in the differential expression between the tumour and surrounding liver throughout the culture for most of the CRs analysed. The only exception was IDO1 which showed a significant decrease in expression on day 5 compared to the levels at the beginning of the culture (Supplementary Figure S2). In conclusion, these results suggest that key immunological features are preserved in the culture of tumour slices.

PCTS are suitable for drug screening of chemo- and immunotherapeutic strategies

After establishing the optimal culture conditions for liver cancer PCTS, we assessed their suitability for drug testing. Firstly, we evaluated the treatment response of a chemotherapeutic used for the locoregional treatment of HCC, doxorubicin (Doxo). The highest concentration of DMSO utilised as vehicle (0.033%) was tested in the slices and found it to be non-toxic (data not shown); therefore subsequent experiments included untreated slices as a control for drug-treated slices. The effect on cell viability, proliferation, and apoptosis of 2 μM Doxo was analysed longitudinally in tumour slices derived from 4 patients with HCC for up to 8 days. The exposure to Doxo induced more than 2-fold increase in LDH release compared to untreated slice cultures (Fig. 5a). Doxorubicin treatment dramatically reduced AEC compared to untreated control slices and at day 5 and 7

---

timepoints and the following parameters analysed for n_{pt} = 2. a | LDH release in the supernatants, shown as OD normalised per slice weight, ratio untreated vs doxo; mean ± SD, n_{PCTS} = 6. b | Adenylate energy charge (AEC) and ATP/mg tissue in a representative slice per timepoint from pt 168. c | Cell proliferation by evaluation of Ki67 staining; mean ± SD, n_{PCTS} = 6. d | Apoptosis by quantification of TUNEL positive nuclei; mean ± SD, n_{PCTS} >6. e | Histological evaluation of H&E staining; n_{PCTS} = 6. f | Stroma analysis of haematoxylin and Sirius red staining; n_{PCTS} = 6. c–f | Representative images are from pt 168, please note some images have been seen in the summary Fig. 3. Scale bars: 100 μm.
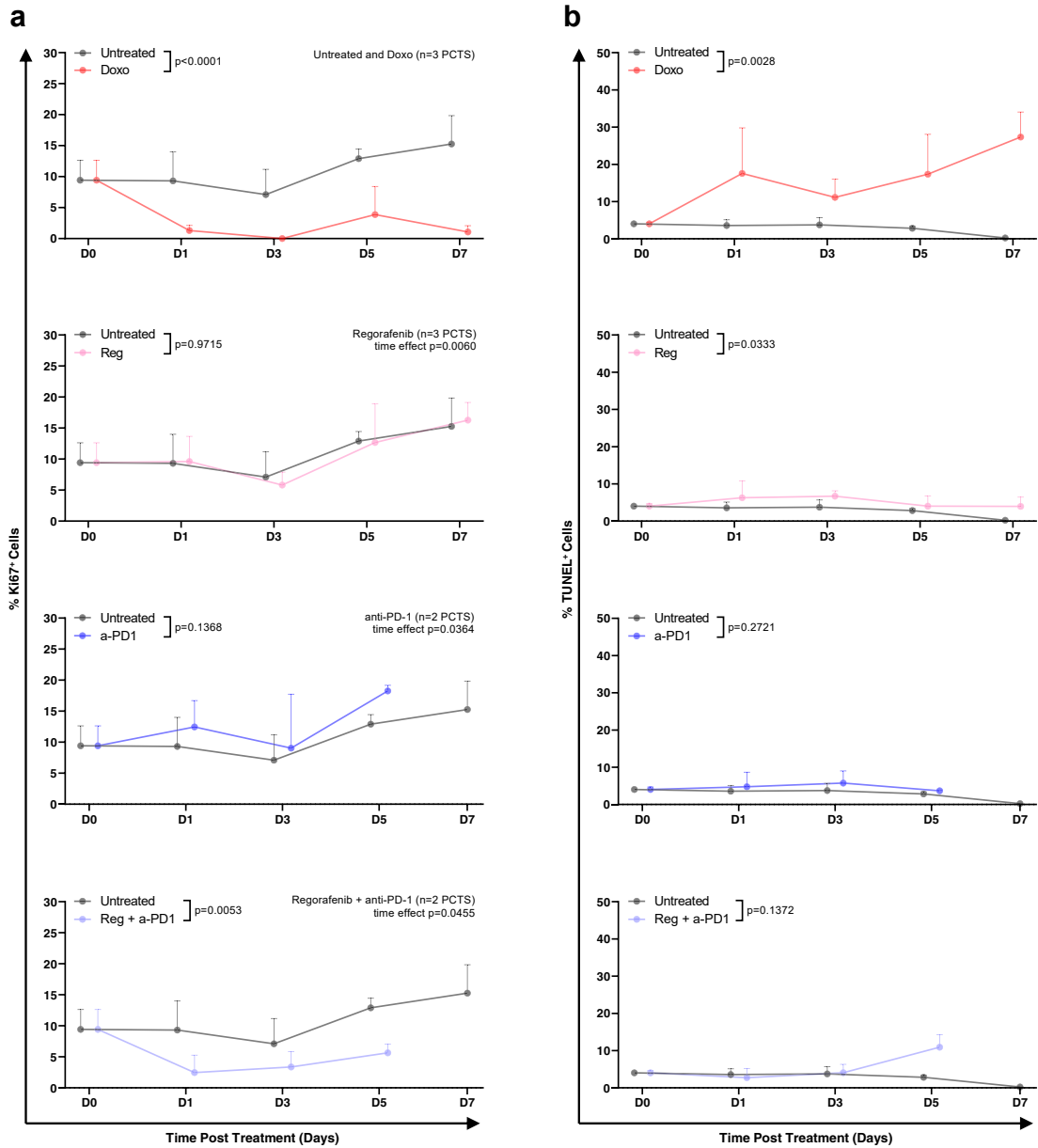
Pt. 168

Fig. 6: **Effect of multi-kinase inhibitor, checkpoint inhibitor (anti-PD1) and combination therapy on PCTS from patient 168: tumour slices had reduced cell proliferation in response to immunotherapy within 8 days of culture.** Tissue slices from pt 168 were treated with doxorubicin (red), anti-PD-1 blocking antibody (blue), regorafenib (pink) and combination therapy (purple) and compared to untreated control (black). The following parameters were assessed in $n_{PCTS} \geq 2$ per timepoint. a | Cell proliferation, shown as percentage of Ki67 positive cells, in PCTS treated with the indicated drugs at the indicated time points; mean ± SD. b | Apoptosis, shown as percentage of TUNEL positive cells, in PCTS treated with the indicated drugs at the indicated timepoints; mean ± SD. Statistical test: 2-way ANOVA.

AEC could not be calculated as the levels of ADP or AMP were undetectable (Fig. 5b). Additionally, there was no ATP detectable for Doxo treated slices, confirming the strong effect on cell viability induced by the

drug (Fig. 5b). Interestingly, the kinetic was variable among patients (pt 168 cell death peak at day 1 and pt 141 at day 3) possibly reflecting differences in response rate. Furthermore, Doxo-treated slices had a significant

Pt. 168
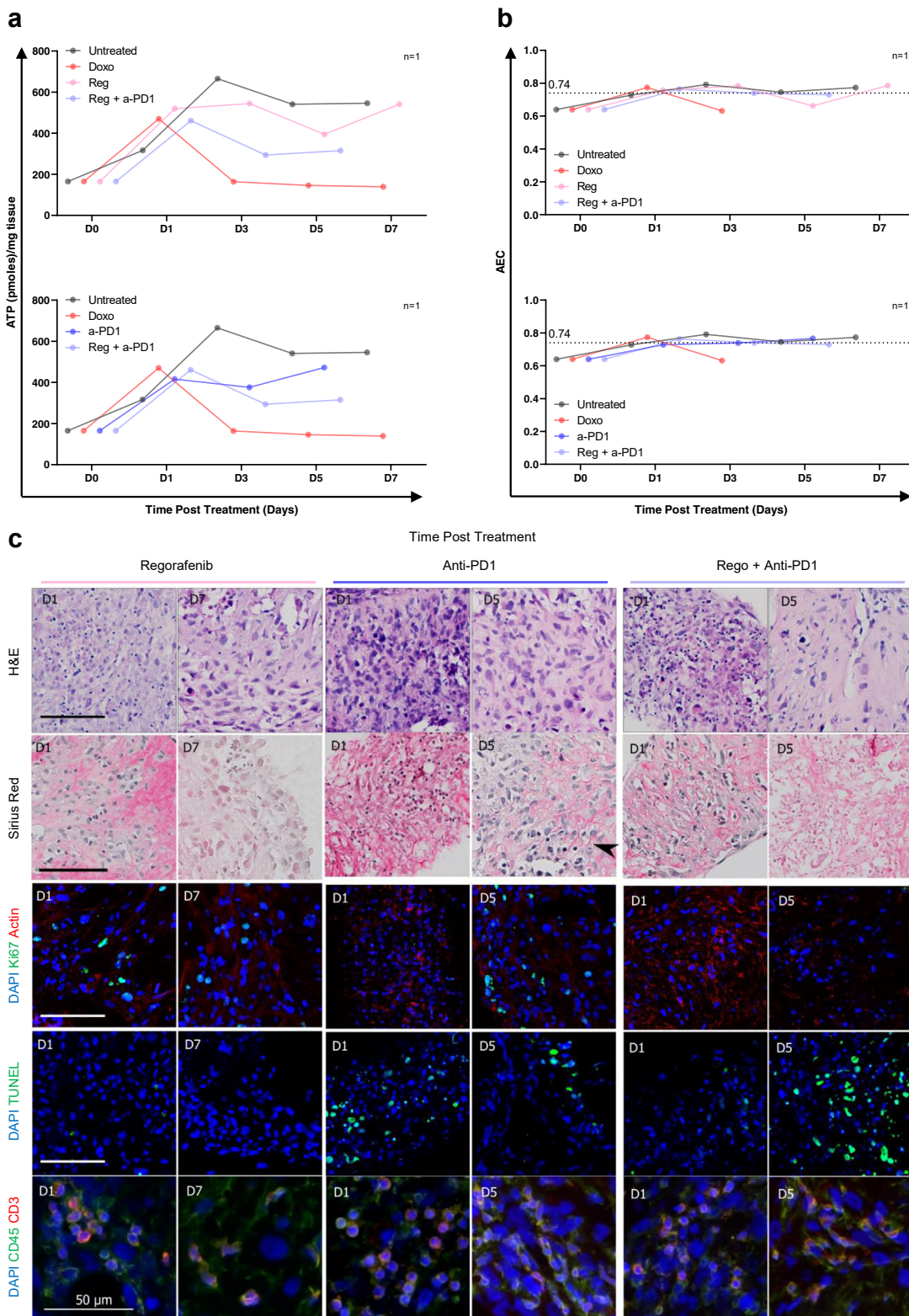
reduction in proliferative capacity (Fig. 5c) and a significant increase in apoptosis compared to untreated slices (Fig. 5d). Following multiple comparisons, Ki67+ cells were significantly reduced at all timepoints from day 1, whilst TUNEL+ cells were significantly increased at days 1, 5 and 7. Changes in Ki67 and TUNEL levels were not observed in the untreated slices, as both the proliferative capacity (Fig. 5c) and the percentage of apoptotic cells (Fig. 5d) remained stable over the duration of the culture. Histological assessment shown that Doxo treatment progressively reduced the presence of viable tumour cells in the tissue slices over time (Fig. 5e). At day 5 there were no more viable tumour cells as indicated by the empty pockets inside the remaining fibrotic stroma (Fig. 5f).

Ultimately, we tested the effect of immunotherapies on the slices, with particular focus on combinatorial treatments used clinically [nivolumab + regorafenib (N + R), nivolumab + ipilimumab (N + R)], including the first line choice for HCC [atezolizumab + bevacizumab) (A + B)][40] and here we report the different response of PCTS to multiple and single-agent therapies in slice cultures derived from two representative patients.

In the HCC-PCTS from patient 168, the results suggested that the combination of regorafenib (Reg) and an anti-PD-1 (a-PD1) blocking antibody may be more effective in reducing cell proliferation when compared to the individual single treatments (Fig. 6a). However, the fraction of apoptotic cells was significantly increased overall, and at day 7 when multiple comparisons were performed, in slices treated with Reg compared to untreated slices (Fig. 6b). The effect of the treatment was further evaluated by the quantification of intracellular ATP, which was lower in the Reg + a-PD1 compared to the single agent (Fig. 7a). The AEC remained constant throughout time and at the same level in both conditions, which suggests that there was no rapid loss of metabolic capacity induced by the therapies (Fig. 7b). H&E demonstrated a clear reduction of tumour epithelial cells after 5 days of treatment with the combination therapy which was not observed for the single treatment (Fig. 7c). The staining of CD3/CD45 showed presence of T-cell infiltrate in all treatment conditions, suggesting an immunocompetent phenotype for this tumour (slices) (Fig. 7c). The response to other combinatorial regimes was then assessed in other slice cultures. In patient 141, treatment with CPIs did not result in a reduction of viable tumour cells, as shown by H&E,

or an increase in tumour cell death TUNEL+ as seen before. However, an overall significant reduction in proliferating tumour cells was observed, as shown by Ki67 staining in PCTS treated with N + I or A + B (Fig. 8a–c). Doxorubicin treatment, used as a positive control, induced a significant decrease of Ki67+ cells and increase in apoptotic cells (Fig. 8a and b).

Discussion

The current study presents the characterisation of an organotypic patient-derived model based on the culture of tumour slices from primary liver cancers. The novelty of this study is the optimisation for extended length of viable PCTS culture *ex vivo* and the longitudinal evaluation of the immune compartment and tumour-specific histological and molecular features. The preservation of these characteristics supports the suitability of PCTS as a platform to investigate both cellular and non-cellular components of the TME. Furthermore, this study also paid particular attention to the generation of slices derived from mixed phenotype HCC-CCA and iCCA tumours. Finally, the drug treatment experiments performed on slices highlight the possibility to use the PCTS as a preclinical tool to screen efficacious therapies for primary liver cancers, including chemotherapeutic or immunotherapeutic approaches.

Whilst the literature extensively covers the feasibility of culturing *ex vivo* slices derived from liver tissue[26–28] and the application of slices originating from various solid tumours has gained momentum in the immune-oncology field,[26,41–44] a study aimed at characterising the PCTS model solely for primary liver cancer and its utilisation in therapeutic development was missing. A few publications have utilised slices for targeted experiments or included sporadic specimens from HCC in cohorts with other tumour types,[45,46] but there was a lack of consensus on the culture parameters of PCTS between different laboratories and differences could be found in medium composition, oxygen concentration and other technical details. It is unclear whether the original tumour features were maintained over time and if the culture had an impact on these characteristics. One of the strengths of the current study is the report of standardised culture conditions (i.e., oxygen partial pressure) for primary liver cancer slices, which we have shown to preserve tumour cell viability and histological heterogeneity over time. The longitudinal evaluation of

Fig. 7: **Effect of multi-kinase inhibitor, checkpoint inhibitor (anti-PD1) and combination therapy on PCTS from patient 168: tumour slices respond to immunotherapy within 8 days of culture.** Tissue slices from pt 168 were treated with doxorubicin (red), anti-PD-1 blocking antibody (blue), regorafenib (pink) and combination therapy (purple) and compared to untreated control (black). The following parameters were assessed in n_PCTS ≥2 per timepoint. a | Weight-adjusted intracellular ATP levels of tissue slices. b | AEC of tissue slices from patient 168 treated with indicated treatment combinations. c | Representative images for H&E, haematoxylin + Sirius red, Ki67, TUNEL, CD45 (leucocytes) and CD3 (T-cells) for treated tissue slices. Scale bars: 100 μm, unless otherwise indicated.

Pt. 141
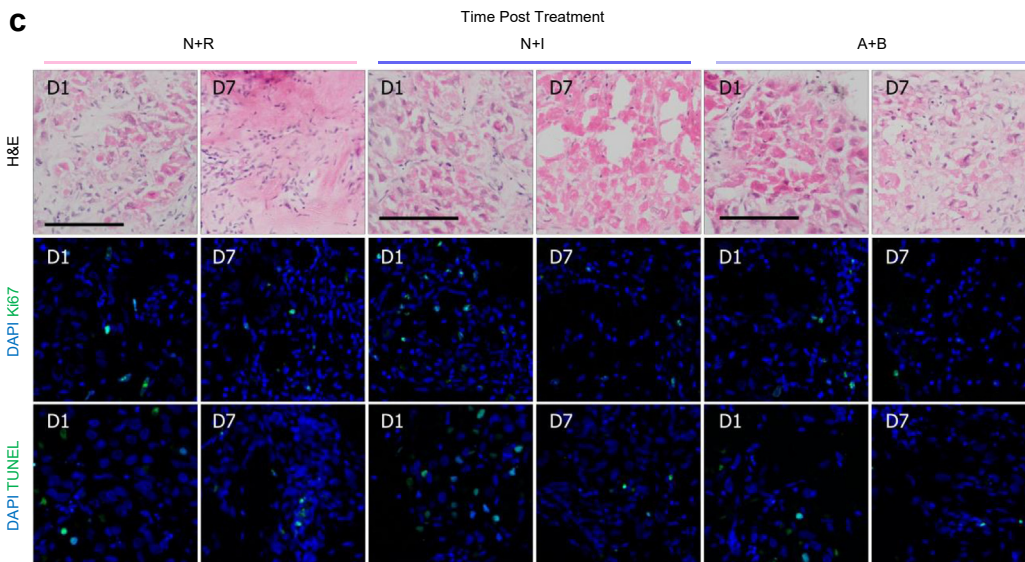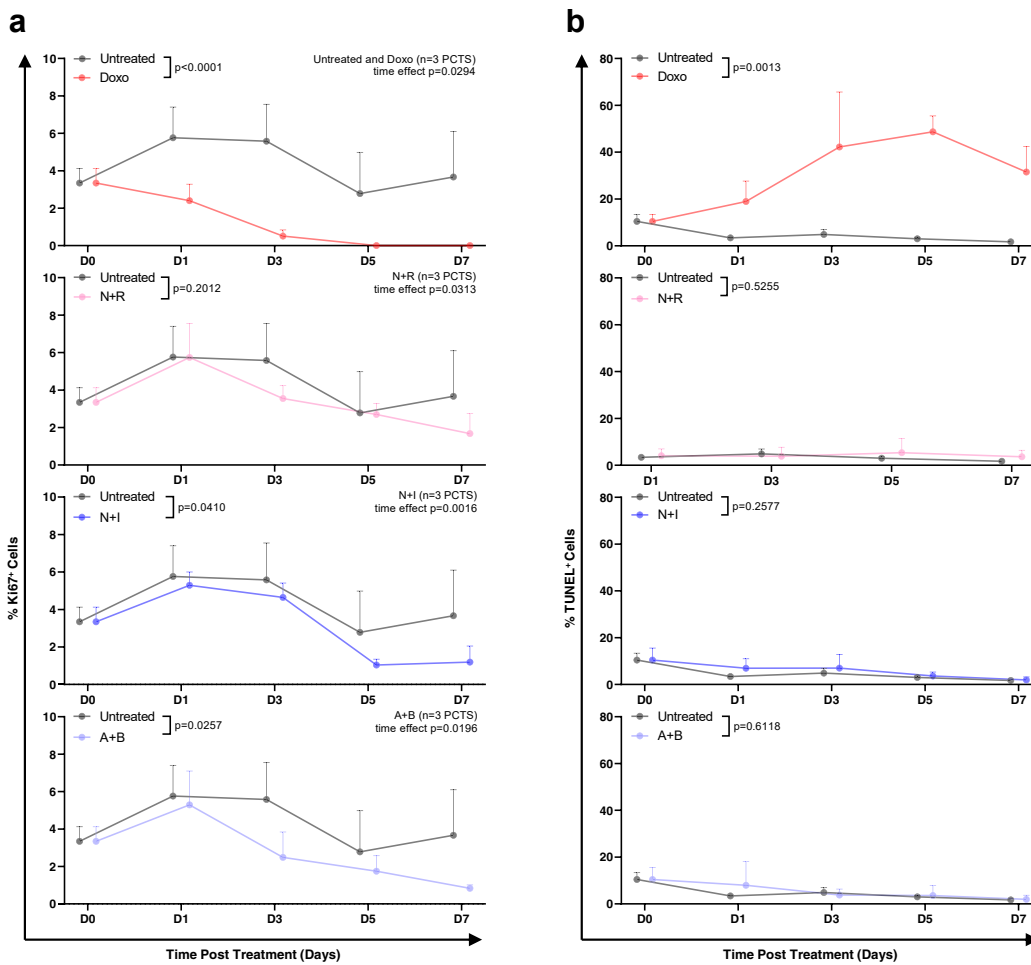
slice weight, LDH and histology provide valuable information regarding the variability among slices and the requirement to combine different methodologies to characterise each culture in order to obtain meaningful results. With regards to tumour proliferation, an advantage of PCTS, compared to other approaches generating cultures from clones, is that tumour cells in the slices retained the original proliferative capacity and growth rate over culture, suggesting the absence of clonal selection. However, we appreciate that this effect may be linked to the relative short-time culture of the slices. Interestingly, this study highlighted the importance of carefully evaluating the effect of oxygen concentration on the tumour slice culture. Unlike tumour-free liver slices,[25,31,47] for tumour slices carbogen seemed to be toxic compared to atmospheric oxygen and caused a reduction of the number of tumour cells in the slices and a decline of Ki67$^+$ proliferating cells. Additionally, the effects of hypoxia on PCTS cultures were explored with the use of the hypoxic mimetic CoCl$_2$. Despite being informative and widely accepted, this method only partially reproduces a "real" hypoxic TME, and this constitutes a limitation of the current study.

Finally, the evaluation of the immune compartment emphasised essential characteristics of the slices relevant for their application in immuno-oncology. PCTS retain a viable and functional immune cell infiltration that can respond to CPI treatment, confirming what was observed in a previous publication for slices generated from syngeneic/PDX mouse tumour models.[45] Moreover, the slices show consistent and stable CR expression throughout the culture. The patient-specific immunophenotype were also preserved in the slices and remarkably, patients 168 and 141 seemed to resemble subtype 1 (immunocompetent) and subtype 3 (immunosuppressive, with high expression of immunosuppressive markers, like PD-1), respectively, according to a novel immunophenotypic classification of HCC recently described.[48] Additional analysis, including spatial transcriptomics or tissue dissociation of PCTS and subsequent immune phenotyping,[45] would allow further characterisation of the cultures to investigate ex vivo the effect of the immunophenotype on treatment response. Indeed, these findings further resonate with the treatment of PCTS using different immunotherapeutic drugs, chemotherapeutics, or combination therapies, highlighting the value of this approach as a personalised

drug screening platform for novel therapeutic strategies targeting the TME or the immune compartment. Despite typically requiring months before therapeutic benefits can be observed in patients following CPI treatment, the slice cultures from both patients showed late signs of disease control, as defined by a reduction in tumour cell proliferation, in response to combination therapies. In support of these findings, a previous report has demonstrated that after 48 h of treatment with anti-PD-L1, tissue slices from HCC murine models had increased frequencies of CD8$^+$ T-cells and increased levels of markers associated with T-cell memory and anti-tumour immunity.[45] Moreover, the capacity to detect varying degrees of response and subsequently correlate these with distinct cellular expression of CRs or soluble factors measurable in the culture supernatants is an important feature of the slice model which could contribute to identify patient-specific markers of response. Nonetheless, a significant constraint of the current work is the restricted number of patient specimens utilised for drug screening. Thus, additional analyses are needed to appraise the effectiveness of the platform more thoroughly.

Finally, HCC patients are at considerable risk of recurrence after liver resection, highlighting the urgent need for therapies to control the disease relapse. As recently demonstrated, combinatorial therapy as an adjuvant before/after liver resection could improve outcomes in HCC patients.[49,50] Again, given the nature of the tissue utilised to obtain slices (tumour and surrounding at resection), studies in PCTS will allow in vitro testing of the efficacy of treatments planned after surgery or investigation into the effects of immuno-therapy on tumour aggressiveness, or lastly, characterisation of the TME where metastases thrive. In all these settings, PCTS represent the ideal system for experimental and preclinical studies and due to the personalised, reliable, and affordable nature of PCTS, the technique is an excellent choice for setting up disease models for rare (liver) tumours.

As with any model, PCTS are not without their limitations. The generation of slices from human tumour tissue is dependent on the availability of freshly resected or explanted human specimens and their efficient transfer from operating theatre to bench. The unpredictability of tissue availability is a common downside to PCTS and all patient-derived models, as it significantly impacts experiment planning and

Fig. 8: Effect of combination therapies with multi-kinase inhibitor and/or checkpoint inhibitors (anti-PD1 and anti-CTLA4) on PCTS from patient 141: tumour slices had reduced cell proliferation in response to immunotherapy within 8 days of culture. Tissue slices from pt 141 were treated with doxorubicin (positive control, red), nivolumab + regorafenib (pink), nivolumab + ipilimumab (blue) and atezolizumab + bevacizumab (purple) for the indicated time and compared to untreated PCTS (black). The following parameters were assessed in n$_{PCTS}$ = 3 per timepoint. a | Cell proliferation: percentage of Ki67 positive cells in tissue slices treated with indicated drug combinations; mean ± SD. b | Apoptosis: percentage of TUNEL positive cells in tissue slices treated with indicated drug combinations; mean ± SD. c | Representative images of H&E, Ki67 and TUNEL staining. Statistical test: 2-way ANOVA. Scale bars: 100 μm.

timelines. Moreover, a quick and effective evaluation of tumour viability is necessary to avoid a waste of time and resources in generating and culturing non-viable slices. A valuable input regarding the quality of the tissue can be obtained with a close collaboration between scientists and experienced histopathologists. Additionally, PCTS may have a variable tumour-to-stroma ratio based on the location of tissue coring but increasing the number of technical replicates can overcome this heterogeneity. Compared to other patient-derived 3D cultures (for example, organoids) which can be expanded *in vitro* and stored long-term, PCTS have a limited life span in culture. Finally, the conservation of multiple patient-specific characteristics results in high levels of inter-experimental heterogeneity, which can make spotting trends, such as the effect of a drug, more difficult, but we believe PCTS better represent real-world patient variability.

In summary, the current study included the optimisation of slice culture conditions, the longitudinal characterisation of PCTS *ex vivo* culture for HCC, iCCA and mixed phenotype, and a drug screening on HCC PCTS of single and combination therapies. The utilisation of the PCTS model has a significant impact on the advancement of disease modelling for primary liver cancer and therefore can open the possibility of developing successful therapeutic approaches for patients affected with these cancers.

References
1   Sung H, Ferlay J, Siegel RL, et al. Global cancer statistics 2020: GLOBOCAN estimates of incidence and mortality worldwide for 36 cancers in 185 countries. *CA Cancer J Clin*. 2021;71(3):209–249.

2   Feng M, Pan Y, Kong R, Shu S. Therapy of primary liver cancer. *Innovation*. 2020;1(2):100032.

3   Ringelhan M, Pfister D, O'Connor T, Pikarsky E, Heikenwalder M. The immunology of hepatocellular carcinoma. *Nat Immunol*. 2018;19(3):222–232.

4   Kudo M. Scientific rationale for combined immunotherapy with PD-1/PD-L1 antibodies and VEGF inhibitors in advanced hepatocellular carcinoma. *Cancers*. 2020;12(5):1089.

5   Voron T, Marcheteau E, Pernot S, et al. Control of the immune response by pro-angiogenic factors. *Front Oncol*. 2014;4:70.

6   Lu LC, Lee YH, Chang CJ, et al. Increased expression of programmed death-ligand 1 in infiltrating immune cells in hepatocellular carcinoma tissues after sorafenib treatment. *Liver Cancer*. 2019;8(2):110–120.

7   Xu F, Jin T, Zhu Y, Dai C. Immune checkpoint therapy in liver cancer. *J Exp Clin Cancer Res*. 2018;37(1):110.

8   Zhang Q, Lou Y, Yang J, et al. Integrated multiomic analysis reveals comprehensive tumour heterogeneity and novel immunophenotypic classification in hepatocellular carcinomas. *Gut*. 2019;68:2019–2031. https://doi.org/10.1136/gutjnl-2019-318912.

9   Clements O, Eliahoo J, Kim JU, Taylor-Robinson SD, Khan SA. Risk factors for intrahepatic and extrahepatic cholangiocarcinoma: a systematic review and meta-analysis. *J Hepatol*. 2020;72(1):95–103.

10   Oh DY, He AR, Qin S, et al. Durvalumab plus gemcitabine and cisplatin in advanced biliary tract cancer. *NEJM Evid*. 2022;1(8) [cited 2022 October 24]. Available from: https://evidence.nejm.org/doi/abs/10.1056/EVIDoa2200015.

11   Finn R. Pembrolizumab as second-line therapy in patients with advanced hepatocellular carcinoma in KEYNOTE-240: a randomized, double-blind, phase III trial. *J Clin Oncol*. 2020;38:193–202.

12   El-Khoueiry AB, Sangro B, Yau T, et al. Nivolumab in patients with advanced hepatocellular carcinoma (CheckMate 040): an open-label, non-comparative, phase 1/2 dose escalation and expansion trial. *Lancet*. 2017;389(10088):2492–2502 [cited 2022 October 18]. Available from: http://www.thelancet.com/article/S0140673617310462/fulltext.

13   Yau T, Park JW, Finn RS, et al. Nivolumab versus sorafenib in advanced hepatocellular carcinoma (CheckMate 459): a randomised, multicentre, open-label, phase 3 trial. *Lancet Oncol*. 2022;23(1):77–90 [cited 2022 October 24]. Available from: http://www.thelancet.com/article/S1470204521006045/fulltext.

14   Finn RS, Qin S, Ikeda M, et al. Atezolizumab plus bevacizumab in unresectable hepatocellular carcinoma. *N Engl J Med*. 2020;382(20):1894–1905 [cited 2022 October 24]. Available from: https://www.nejm.org/doi/10.1056/NEJMoa1915745.

15   Hay M, Thomas DW, Craighead JL, Economides C, Rosenthal J. Clinical development success rates for investigational drugs. *Nat Biotechnol*. 2014;32(1):40–51. https://doi.org/10.1038/nbt.2786.

16   Finn RS, Qin S, Ikeda M, et al. IMbrave150: updated overall survival (OS) data from a global, randomized, open-label phase III study of atezolizumab (atezo) + bevacizumab (bev) versus sorafenib (sor) in patients (pts) with unresectable hepatocellular carcinoma (HCC). *J Clin Oncol*. 2021;39(3_suppl):267. https://doi.org/10.1200/JCO.2021.39.3_suppl.267.

17   Richmond A, Su Y. Mouse xenograft models vs GEM models for human cancer therapeutics. *Dis Model Mech*. 2008;1(2–3):78–82.

18   Mestas J, Hughes CCW. Of mice and not men: differences between mouse and human immunology. *J Immunol*. 2004;172:2731–2738 [cited 2022 November 17]. Available from: http://journals.aai.org/jimmunol/article-pdf/172/5/2731/1181081/2731.pdf.

19   Bernard D, Peakman M, Hayday AC. Establishing humanized mice using stem cells: maximizing the potential. *Clin Exp Immunol*. 2008;152(3):406–414.

20   Kudo M. Why does every hepatocellular carcinoma clinical trial using molecular targeted agents fail? *Liver Cancer*. 2012;1(2):59–60. Available from: https://pubmed.ncbi.nlm.nih.gov/24159572.

21   Paul SM, Mytelka DS, Dunwiddie CT, et al. How to improve RD productivity: the pharmaceutical industry's grand challenge. *Nat Rev Drug Discov*. 2010;9:203–214.

22   Broutier L, Mastrogiovanni G, Verstegen MM, et al. Human primary liver cancer-derived organoid cultures for disease modeling and drug screening. *Nat Med*. 2017;23(12):1424–1435.

23   Sükei T, Palma E, Urbani L. Interplay between cellular and non-cellular components of the tumour microenvironment in hepatocellular carcinoma. *Cancers*. 2021;13:5586.

24   Fujii M, Shimokawa M, Date S, et al. A colorectal tumor organoid library demonstrates progressive loss of niche factor requirements during tumorigenesis. *Cell Stem Cell*. 2016;18(6):827–838.

25 De Graaf IAM, Olinga P, De Jager MH, et al. Preparation and in-cubation of precision-cut liver and intestinal slices for application in drug metabolism and toxicity studies. *Nat Protoc*. 2010;5(9):1540–1551. https://doi.org/10.1038/nprot.2010.111.

26 Dewyse L, Reynaert H, van Grunsven LA. Best practices and progress in precision-cut liver slice cultures. *Int J Mol Sci*. 2021;22(13):7137.

27 Palma E, Doornebal EJ, Chokshi S. Precision-cut liver slices: a versatile tool to advance liver research. *Hepatol Int*. 2019;13(1):51–57.

28 Paish HL, Reed LH, Brown H, et al. A bioreactor technology for modeling fibrosis in human and rodent precision-cut liver slices. *Hepatology*. 2019;70(4):1377–1391.

29 Doornebal EJ, Harris N, Riva A, et al. Human immunocompetent model of neuroendocrine liver metastases recapitulates patient-specific tumour microenvironment. *Front Endocrinol*. 2022;13: 909180 [cited 2023 March 17]. Available from: http://pmc/articles/PMC9326114.

30 de Graaf IAM, Olinga P, de Jager MH, et al. Preparation and in-cubation of precision-cut liver and intestinal slices for application in drug metabolism and toxicity studies. *Nat Protoc*. 2010;5(9):1540–1551.

31 Palma E, Riva A, Moreno C, et al. Perturbations in mitochondrial dynamics are closely involved in the progression of alcoholic liver disease. *Alcohol Clin Exp Res*. 2020;44(4):856–865.

32 Dubbelboer IR, Pavlovic N, Heindryckx F, Sjögren E, Lennernäs H. Liver cancer cell lines treated with doxorubicin under normoxia and hypoxia: cell viability and oncologic protein profile. *Cancers*. 2019;11(7):1024.

33 Sadeghi-Aliabadi H, Minaiyan M, Dabestan A. Cytotoxic evaluation of doxorubicin in combination with simvastatin against human cancer cells. *Res Pharm Sci*. 2010;5(2):127–133.

34 Carr BI, Cavallini A, Lippolis C, et al. Fluoro-Sorafenib (Regor-afenib) effects on hepatoma cells: growth inhibition, quiescence, and recovery. *J Cell Physiol*. 2013;228(2):292–297.

35 Carr BI, Alessandro RD, Refolo MG, et al. Effects of low concen-trations of regorafenib and sorafenib on human HCC cell AFP, migration, invasion and growth in vitro Brian. *J Cell Physiol*. 2014;228(6):1344–1350.

36 Wang C, Thudium KB, Han M, et al. In vitro characterization of the anti-PD-1 antibody nivolumab, BMS-936558, and in vivo toxicology in non-human primates. *Cancer Immunol Res*. 2014;2(9):846–856.

37 Li D, Li J, Chu H, Wang Z. A functional antibody cross-reactive to both human and murine cytotoxic T-lymphocyte-associated protein 4 via binding to an N-glycosylation epitope. *MAbs*. 2020;12(1): 1725365.

38 Yang J, Wang Q, Qiao C, et al. Potent anti-angiogenesis and anti-tumor activity of a novel human anti-VEGF antibody, MIL60. *Cell Mol Immunol*. 2014;11(3):285–293.

39 Herbst RS, Soria JC, Kowanetz M, et al. Predictive correlates of response to the anti-PD-L1 antibody MPDL3280A. *Nature*. 2016;515(7528):563–567.

40 D'Alessio A, Fulgenzi CAM, Nishida N, et al. Preliminary evidence of safety and tolerability of atezolizumab plus bevacizumab in pa-tients with hepatocellular carcinoma and Child-Pugh A and B cirrhosis: a real-world study. *Hepatology*. 2022;76(4):1000–1012. https://doi.org/10.1002/hep.32468.

41 Dimou P, Trivedi S, Liousia M, D'souza RR, Klampatsa A. Preci-sion-cut tumor slices (PCTS) as an ex vivo model in immuno-therapy research. *Antibodies*. 2022;11(2):26 [cited 2022 October 27]. Available from: https://pubmed.ncbi.nlm.nih.gov/35466279/.

42 He L, Deng C. Recent advances in organotypic tissue slice cultures for anticancer drug development. *Int J Biol Sci*. 2022;18(15):5885–5896 [cited 2022 October 27]. Available from: https://pubmed.ncbi.nlm.nih.gov/36263166/.

43 Mackenzie NJ, Nicholls C, Templeton AR, et al. Modelling the tu-mor immune microenvironment for precision immunotherapy. *Clin Transl Immunol*. 2022;11(6):e1400 [cited 2022 October 27]. Available from: https://pubmed.ncbi.nlm.nih.gov/35782339/.

44 Sompel K, Smith AJ, Hauer C, et al. Precision cut lung slices as a preclinical model for non–small cell lung cancer chemopreven-tion. *Cancer Prev Res*. 2023;116(5):247–258 [cited 2023 May 15]. Available from: https://aacrjournals.org/cancerpreventionresear ch/article/16/5/247/725946/Precision-Cut-Lung-Slices-as-a-Preclin ical-Model.

45 Sivakumar R, Chan M, Shin JS, et al. Organotypic tumor slice cultures provide a versatile platform for immuno-oncology and drug discovery. *OncoImmunology*. 2019;8(12):e1670019.

46 Zimmermann M, Armeanu S, Smirnow I, et al. Human precision-cut liver tumor slices as a tumor patient-individual predictive test system for oncolytic measles vaccine viruses. *Int J Oncol*. 2009;34(5):1247–1256.

47 Westra IM, Mutsaers HAM, Luangmonkong T, et al. Human precision-cut liver slices as a model to test antifibrotic drugs in the early onset of liver fibrosis. *Toxicol In Vitro*. 2016;35:77–85.

48 Zhang Q, Lou Y, Yang J, et al. Integrated multiomic analysis reveals comprehensive tumour heterogeneity and novel immunophenotypic classification in hepatocellular carcinomas. *Gut*. 2019;68(11):2019–2031 [cited 2022 October 27]. Available from: https://pubmed.ncbi.nlm.nih.gov/31227589/.

49 Pinato DJ, Cortellini A, Sukumaran A, et al. PRIME-HCC: phase Ib study of neoadjuvant ipilimumab and nivolumab prior to liver resection for hepatocellular carcinoma. *BMC Cancer*. 2021;21(1):301.

50 Kudo M. Adjuvant atezolizumab-bevacizumab after curative ther-apy for hepatocellular carcinoma. *Hepatobiliary Surg Nutr*. 2023;12(3):435–439.